Intramyocardial protein therapy with vascular endothelial growth factor (VEGF-165) induces functional angiogenesis in rat senescent myocardium.

Sophie Besse, François Boucher, Gilberte Linguet, Laurent Riou, Joël de Leiris, Bertrand Riou, Julien Dimastromatteo, René Comte, José Courty, Jean Delbe

JOURNAL OF PHYSIOLOGY AND PHARMACOLOGY 2010, 61, 6, 651-661
www.jpp.krakow.pl

Original articles

S. BESSE[1,2], F. BOUCHER[3], G. LINGUET[1], L. RIOU[4], J. DE LEIRIS[3], B. RIOU[5], J. DIMASTROMATTEO[4], R. COMTE[1], J. COURTY[1], J. DELBE[1]

INTRAMYOCARDIAL PROTEIN THERAPY WITH VASCULAR ENDOTHELIAL GROWTH FACTOR (VEGF-165) INDUCES FUNCTIONAL ANGIOGENESIS IN RAT SENESCENT MYOCARDIUM

[1]Laboratoire Croissance Cellulaire, Reparation et Regeneration Tissulaires, EAC CNRS 7149, Universite Paris-Est, Creteil, France; [2]Universite Paris-Descartes, Paris, France; [3]Laboratoire PRETA-TIMC-IMAG, UMR CNRS 5525, Universite Joseph Fourier, La Tronche, France; [4]INSERM U877 Radiopharmaceutiques Biocliniques, Universite J. Fourier, La Tronche, France; [5]UMRS INSERM 956, Universite Pierre et Marie Curie-Paris 6 and Service d'Accueil des Urgences, CHU Pitie-Salpetriere, Assistance Publique-Hopitaux de Paris, Paris, France

Myocardial capillary density and angiogenesis are impaired during aging but whether growth factor therapy is able to induce functional neovascularization in senescent heart have never been studied. In 3, 24, 28 and 32 mo male Wistar rats, cardiac hemodynamic measurements indicated heart failure at 28 and 32 mo, associated with left ventricular hypertrophy. VEGF/VEGF-R2, Ang-1/Ang-2/Tie-2 and PTN levels, quantitated in left ventricle by western blotting and immunohistochemistry, showed that VEGF and VEGF-R2 levels were specifically decreased during aging. *In vitro* angiogenesis±rhVEGF-165 (5 and 50 ng/mL) was measured in aortic segments in 3D-collagen. Aortic sprouting was decreased during aging but restored by VEGF treatment ($P<0.001$), similarly in 3 and 24 mo with 50 ng/mL VEGF. Finally, 3 and 24 mo rats were submitted to *in vivo* intramyocardial rhVEGF-165 (10 micrograms) or saline solution injection and angiogenesis was measured by SPECT imaging of the alpha(v)beta(3) integrin-targeted tracer (99m)Tc-RAFT-RGD, capillary fluorescence staining in isolated perfused heart and vWF and alpha smooth muscle actin immunohistochemistry, 7 and 21 days later. VEGF administration increased capillary density in 3 but also in 24 mo rats at days 7 (+26%, $P<0.01$) and 21 (+41%, $P<0.01$) and arteriolar density at day 21 (+36%, $P<0.01$). Activity of (99m)Tc-RAFT-RGD and capillary fluorescence labeling indicated that new formed capillaries were functional. Cardiac aging was associated with strong VEGF/VEGF-R2 pathway downregulation. VEGF-165 protein therapy was able to induce *in vitro* and *in vivo* angiogenesis during aging. In 24 mo hearts, *in vivo* angiogenesis was functional, sustained and comparable to neovascularization observed in 3 mo hearts.

Key words: *aging, myocardium, protein therapy angiogenesis, vascular endothelial growth factor, cardiac hypertrophy, heart failure*

INTRODUCTION

Advanced age is a risk factor for cardiovascular disease and congestive heart failure is the major cause of hospitalizations and death of persons older than 65 years (1). The cardiovascular aging process in animals and human subjects is characterized by endothelial dysfunction resulting from oxidative stress associated with an impairment of coronary perfusion and reserve which might facilitate the myocyte loss, fibrosis and subsequently reduce heart function, both leading to a particular vulnerability to cardiovascular events such as ischemia-reperfusion (2-4). Major part of coronary perfusion results from capillaries and consequently angiogenesis, *i.e.* the sprouting of new blood vessels from a preexisting capillary network, is essential for the repair of heart tissue. Unfortunately different studies reported an age-associated impairment of angiogenesis (5, 6).

Angiogenesis, resulting from endothelial proliferation, migration and capillary tube-like formation, is regulated by many diffusible, inducible and inhibitory angiogenic factors, such as vascular endothelial growth factor (VEGF), angiopoietins (Ang-1 and Ang-2) and pleitrophin (PTN) (7, 8). In the myocardium, the involvement of the angiogenic growth factor/receptor regulatory systems Ang-1/Ang-2/Tie-2 and VEGF/VEGF-R2 in the growth of coronary vasculature have been well established (8, 9). Consequently, therapeutic approaches have been aimed at promoting cardiac angiogenesis by growth factor therapy in different pathophysiological animal models (10-12). Among growth factors, VEGF plays a pivotal role in angiogenesis since it stimulates proliferation and migration of endothelial cells and triggers a series of event inducing new blood vessel growth, through its main receptor VEGF-R2 (7, 9, 13). Moreover, cardiac VEGF therapies improved global and regional LV function in different pathological states (10, 12, 14, 15).

In senescent rodent heart, PDGF-A and -B are reduced (11) as well as VEGF and its main receptor VEGF-R2 (16, 17). Moreover, the Edelberg group' s studies reported a successful

cardiac therapy during aging with PDGF-AB which induced angiogenesis and improved myocardial function after myocardial infarction (11, 18). However in senescent hearts, to our knowledge no further study investigating a protein therapy with other growth factors, is currently available.

In the present study, we investigated during aging the time course of protein expression of main growth factors involved in angiogenesis during aging and identified VEGF/VEGF-R2 as the unique down-regulated angiogenic growth factor/receptor regulatory system in the senescent heart. We then tested the hypothesis that VEGF protein therapy was able to restore during aging 1) capillary outgrowth in an *in vitro* model of aortic sprouting and 2) coronary angiogenesis in an *in vivo* rat model. The results might provide important guidelines and rationales for selections of angiogenic/arteriogenic factors for future clinical trials in elderly patients.

MATERIALS AND METHODS

Animals

Investigations were conducted with 3, 24, 28 and 32 month old (mo) male Wistar rats (Charles River Laboratories, France) in accordance with the Guide for the Care and Use of Laboratory Animals published by the US National Institutes of Health (NIH Publication No. 85-23, revised 1996) and with the regulations of the official edict of the French Ministry of Agriculture. Mortality in the male Wistar rat population is 50% at 24 mo, 70% at 28 mo and 92% at 32 mo. In rats, 24 mo corresponds to 70-75 years in humans (19).

Hemodynamic measurements

Hemodynamic variables were measured using a Mikro-Tip® Pressure catheter (Millar Instruments Inc, HSE, Germany) in anesthetized 3 (n=8), 24 (n=12), 28 (n=12) and 32 (n=10) mo rats as previously reported (20). Left ventricular systolic pressure (LVSP), left ventricular end-diastolic pressure (LVEDP), positive (+LVdP/dt) and negative (-LVdP/dt) first derivative for maximal rates of left ventricular pressure development were recorded. After heart excision, left ventricle with septum (LV) and right ventricle were weighted. LV were then frozen in liquid nitrogen for growth factor quantification, or in Tissue-Tek O.C.T. Compound (Sakura Finetek, USA) for immunohistochemistry.

Production of recombinant human VEGF protein

Recombinant human $VEGF_{165}$ ($rhVEGF_{165}$) protein was produced in Sf9 insect cells with the recombinant baculovirus expression system (21). Briefly Sf9 insect cells were grown and infected with recombinant vector at 28°C in GIBCO Sf-900™ III serum free medium (Invitrogen, France), supplemented with penicillin and streptomicin (500 U/ml). Protein purification was then performed by cation exchange and heparin-affinity chromatography. Biological activity of $rhVEGF_{165}$ was tested on human umbilical vein endothelial cells proliferation

Quantification of growth factors and their receptors Western blotting analysis and VEGF Elisa

For Ang-1 and Ang-2 quantification in LV, protein extraction was performed as previously reported (22). Fifty µg of total proteins were separated on 10% SDS-PAGE and electrophoretically blotted onto polyvinylidenefluoride membranes (Immobilon P, Millipore, France). After blocking in 5% non fat dry milk in PBS, membranes were incubated for 90 min with a goat anti-Ang-2 or anti-Ang-1 antibody (1:100; Santa Cruz Biotechnology Inc., Germany) in PBS with 5% dry milk and 0.2% Tween. For PTN quantification, LV samples were homogenized in 20 mM Hepes, pH 7.4, 2M NaCl, 1 µg/ml aprotinin, leupeptin and pepstatin (Sigma-Aldrich, France), 0.1 mM PMSF, 3 mM EDTA. After centrifugation, 600 µg of proteins in 20 mM HEPES, 0.6M NaCl were incubated overnight at 4°C with heparin-Sepharose CL-6B beads (Amersham Pharmacia Biotech., France) on a rotating rack and treated as previously described (23). Nonspecific binding was prevented by incubating the membrane in SuperBlock® Blocking Buffer (Thermo-scientific Pierce Protein Research, Rockford, USA) for 20 min. The membranes were then incubated overnight at 4°C with goat anti-PTN antibody (R&D systems Europe, ref. AF-252-PB, Lille, France) at 1:1000 dilution in PBS-Tween 0.2% with 1/30 SuperBlock® Blocking Buffer and then washed in PBS-Tween 0.2%.

For all membranes, bound antibodies were visualized with incubation with peroxidase-conjugated rabbit anti-goat IgG (1/10000, Jackson ImmunoResearch, United Kindom). After incubation with a chemoluminescent reagent (chemoluminescent Detection System Kit; Chemicon International Inc., USA), membranes were exposed to Kodak Biomax light films. Intensity of Ang-1, Ang-2 and PTN bands was determined by scanning densitometry (MetaMorph 7.0, Molecular Devices, USA) and normalized to the densitometric score of a control LV sample, added in all blots.

Concentrations of VEGF in LV were measured using RayBio® Rat VEGF ELISA kit (RayBiotech Inc., USA).

Immunohistochemistry

Hearts were cut transversally from apex to base and 10 sections (7 µm thickness) were immunostained with antibodies against VEGF-R1, VEGF-R2, Tie-1 and Tie-2. After fixation in ice-cold acetone (20 min) and quenching of endogenous biotins (Avidin/Biotin Blocking Kit, Vector Laboratories), sections were incubated with rabbit polyclonal antibodies against VEGF-R1 and VEGF-R2 (1:100; Santa Cruz Biotechnology Inc.) and rabbit polyclonal antibodies against Tie-1 and Tie-2 (1:50, Santa Cruz Biotechnology Inc.) at room temperature for 90 min. Sections were then serially incubated with biotin-conjugated anti-rabbit second antibody (1:1000; Jackson ImmunoResearch) for 45 min and with VECTASTAIN® ABC-AP Reagent (Vector Laboratories) and alkaline phosphatase substrate solution (VECTOR® Red substrate kit, Vector Laboratories), according to manufacturer's instructions. Negative controls were performed using rabbit IgGs instead of primary antibodies. Digital images of immunostained sections were acquired using a Nikon microscope. Quantitative mesurements of the different labellings was processed by a computerized image analyzer (MetaMorph 7.0).

In vitro angiogenesis

Angiogenesis was studied by culturing rings of rat aorta in 3-dimensional collagen gels. Thoracic aortas were removed from 3 and 24 mo rats and 1-2 mm-long aortic rings were sectioned and embedded in 2 mL of collagen gel as previously described (24). Aortic rings were maintained at 37°C in DMEM + 10% fetal calf serum (PAA) + 50 µg/mL gentamycine (Invitrogen, France). At day 0 and 3, saline solution (control) or 5 or 50 ng/mL of $rhVEGF_{165}$ were added to the culture medium of 3 (n=12, n=8 and n=12 respectively) and 24 (n=10, n=12 and n=12 respectively) mo rings. Rings were photographied at day 3 and 6 by phase contrast microscopy. Image analysis was processed by

a computerized image analyzer (MetaMorph 7.0) allowing the measurement of endothelial cell number and maximal microvessel length from the aortic explant.

In vivo angiogenesis

Surgical procedure

Three and 24 mo rats were anesthetized (0.5% isoflurane) and mechanically ventilated, and a left thoracotomy was performed, enabling injection into the inferior half of the LV free wall in 5 points according to *Fig. 1*. Into each of the 5 sites, 4 µl of 0.5 µg/µl of $rhVEGF_{165}$ in saline solution or of saline solution alone (control groups) were injected using Hamilton syringe with 30-gauge needle. Tissue distribution and retention of injected growth factors with intramyocardial injection compared favorably with other routes of administration and the injected products had sufficient diffusion to induce improvement of cardiac function and/or perfusion (25). The dose of $rhVEGF_{165}$ was based on a previous study with the myocardial infarction model (26). To know how long the $rhVEGF_{165}$ persisted in the heart after treatment, immunofluorescence staining of human $VEGF_{165}$ was performed with the monoclonal antibody presenting the lowest cross-reactivity with rat VEGF (R&D system, MAB293) but unfortunately such antibody also recognized VEGF from rat origin which did not allow determine if rhVEGF165 persisted or was degraded after 7 and 21 days of treatment.

Three mo and 24 mo-control and 3 and 24 mo-VEGF rats were submitted, 7 (n=9 and n=8 and n=10 and n=13 respectively) and 21 (n=8 and n=8 and n=8 and n=9 respectively) days after treatment, to *in vivo* noninvasive dual-isotope imaging or to *in situ* fluorescence staining of perfused capillaries and hearts were arrested in diastole with 18 mM potassium chloride and frozen as described above for immunohistochemistry.

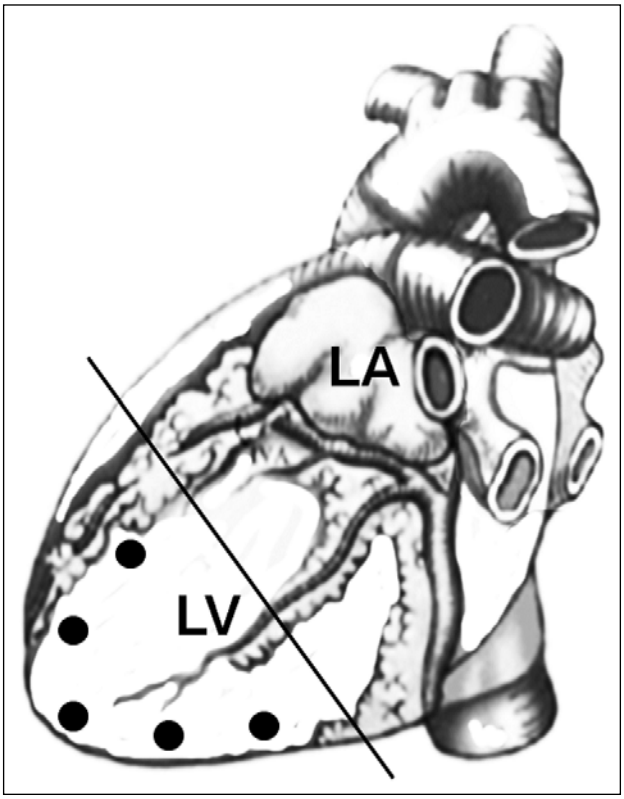

Fig. 1. Localisation of intramyocardial injection sites. The $rhVEGF_{165}$ (10 µg in 20 µL) or saline solution (20 µL) were injected in the inferior half of the left ventricular free wall (black circle) of 3 and 24 mo rat hearts. LA: left atrium; LV: left ventricle.

In vivo noninvasive dual-isotope imaging

Seven and 21 days after surgery, the myocardial perfusion agent ^{201}Thallium (57.8±4.5 MBq) and the $\alpha_v\beta_3$-specific tracer ^{99m}Tc-RAFT-RGD (142.0±8.5 MBq) were injected into the saphenous vein of anesthetized rats (27). Thirty minutes later, the animals were submitted to *in vivo* dual-isotope myocardial pinhole SPECT imaging for 120 min using a small animal γ-camera (γ-imagerS, BiospaceLab). The window settings were 125-150 keV and 55-85 keV for ^{99m}Tc and ^{201}Thallium, respectively and decay correction was automatically applied to the recorded Tc-99m and Tl-201 image counts. Pilot phantom experiments demonstrated minimal (<5%) isotope cross-talk. The energy resolution of the gamma imager is 11% at 140 keV and 20% at 71 keV, implying that the full width at half maximum is 15.4 keV and 14.2 keV for Tc-99m and Tl-201, respectively. With the emission energy difference between Tc-99m and Tl-201 being 69 keV that is, approximately 4.5-fold the full width at half maximum of both Tc-99m and Tl-201 peaks. Image reconstruction was performed using γ-acquisition$^+$ software (BiospaceLab, France) and an Ordered-Subsets-Expectation-Maximization reconstruction algorithm. One mm-thick consecutive short-axis slices (10/animal) were generated from base-to-apex, using Amira software (Visage Imaging GmbH, Germany). These 2D, dual-isotope extracted slices were analyzed using γ-vision-software (BiospaceLab). ^{99m}Tc-RAFT-RGD activity in hot spots, detected within the LV free wall delineated with ^{201}Thallium images and corresponding to sites of intramyocardial $rhVEGF_{165}$ or saline solution injections, was quantified and compared to ^{99m}Tc-RAFT-RGD septal activity (LV/S ratio). Thallium-201 was exclusively used for the anatomical delineation of LV volume. Therefore, changes in myocardial activity due to tracer washout over the image acquisition period and potential modest variations in regional myocardial tracer kinetics due to changes in vascular permeability following $rhVEGF_{165}$ injection did not represent a major bias in the present study (28, 29).

In situ fluorescence staining of perfused capillaries

Isolated hearts were perfused according to Langendorff as previously described (3). After 15 min of equilibration, hearts were perfused with Krebs-Henseleit solution containing 0.02% fluorescein-isothiocyanate-conjugated (FITC) lycopersicon esculentum lectin (Sigma-Aldrich), an endothelial cell specific marker (10). After rinsing, hearts were perfused with FineFIX fixative (Milestone, Kalamazoo, USA), fixed overnight and prepared for frozen cross-sections (7 γm thickness). Nuclei were counterstained with blue fluorescent 4',6-diamidino-2-phenylindole (DAPI; 1:4000, Sigma-Aldrich) and sections were mounted in ImmunoMount (Shandon Inc., USA). Green (FITC) and blue (DAPI) fluorescent images of endocardial region of 20 transversal sections between the apex and the middle left ventricle were captured using an Olympus fluorescence microscope.

Immunostaining of capillaries and arterioles

After fixation of myocardial sections in ice-cold acetone for 20 min, 10 transversal sections between the apex and the middle left ventricle were immunostained with antibodies against von Willebrand Factor (vWF) and alpha smooth muscle actin (α sma). For vWF immunostaining, after quenching with endogenous

peroxidases with hydrogen peroxide (0.3%), sections were incubated with a rabbit polyclonal antibody against vWF (1:200 Dako France SAS, France) for 1 hour. Sections were then serially incubated with biotin-conjugated anti-rabbit second antibody (1:1000; Jackson ImmunoResearch) for 40 min and with streptoavidin-peroxidase (Vectastain® Elite® ABC Kit, Vector Laboratories) and diaminobenzidine-Nickel (DAB substrate kit for peroxidase, Vector Laboratories), according to manufacturer's instructions.

For α sma immunostaining, after quenching of endogenous biotins (Avidin/Biotin Blocking Kit, Vector Laboratories), sections were incubated with a mouse monoclonal antibody against α sma (1:50; Dako France SAS) for 1 hour. Sections were then serially incubated with biotin-conjugated anti-mouse second antibody (1:1000; Dako France SAS) for 45 min and treated with VECTASTAIN® ABC-AP Reagent and alkaline phosphatase substrate solution as described above. Negative controls were performed using rabbit IgGs and mouse IgG instead of anti-vWF of anti-α sma primary antibodies respectively. Immunolabelled sections were photographied using a Nikon microscope. Image analysis was processed by a computerized image analyzer (MetaMorph 7.0) allowing quantification of capillary and arteriolar densities and numbers. Capillaries surface and number were quantitated by vWF immunostaining. All discrete clusters or single cells stained for vWF, with or without lumen, were counted as a vessel. Arterioles were quantitated using the following criteria: 1) positive for α sma 2) having a visible lumen and 3) a diameter between 10 and 100 μm.

Statistical analysis

Data were expressed as mean±S.E.M. Statistical analysis was performed using one-way analysis of variance and between group, comparison was performed using a Newman-Keuls test. All P values were two-tailed and $P<0.05$ was considered significant.

RESULTS

Cardiac hypertrophy and heart failure at advanced age

The left ventricular to right ventricular weight ratio (LVW/RVW) and hemodynamic variables were not significantly different between 3 mo and 24 mo rats (*Table 1*). In contrast, an age-dependent increase in LVW/RVW was observed at 28 mo together with a decrease in LVSP, +LVdP/dt and -LVdP/dt and an increase in LVEDP (*Table 1*). Both the LV hypertrophy and LV function impairment gave evidence of heart failure at these advanced ages. The severity of heart failure increased between 28 and 32 months of age (*Table 1*). For a matter of fact, surgical procedure in 28 mo rat for $rhVEGF_{165}$ as well as control treatment increased dramatically post-operative mortality (80% *vs.* 15% in 24 mo rats) and consequently did not allow to determine the effects of *in vivo* therapy with $rhVEGF_{165}$ in these advances ages (datas not shown).

Aging strongly impaired cardiac VEGF pathways

Ang-2 and PTN levels were similar between 3 and 24 mo groups (*Fig. 2*). In contrast, VEGF and VEGF-R2 levels strongly decreased between 3 and 24 months of age (*Fig. 2* and *3*). Ang-1 level was increased in 24 mo group (+29%; *Fig. 2*) whereas Tie-2 level was unchanged (*Fig. 3*), as compared to 3 mo group. However Ang-1/Ang-2 ratio was not significantly different in 3 and 24 mo hearts (0.73±0.06 *vs.* 0.92±0.08 respectively).

Ang-1 and Ang-2 levels progressively increased between 24 and 32 months of age (*Fig. 2*) without significant changes in Tie-2 levels. In contrast, both VEGF and VEGFR-2 levels were reduced by 75% and 50% respectively at 32 mo, as compared to 3 mo hearts. PTN level was only increased at 32 months of age. VEGF-R1 and Tie-1 immunostainings revealed sparse localization at all ages (data not shown), as previously reported (16, 30). Cardiac aging results in a strong downregulation of VEGF/VEGF-R2 pathway.

Age-dependent decrease in aortic sprouting restored by $rhVEGF_{165}$ administration

In aortic ring model, formed microvessels are constituted by endothelial tubes and surrounding mural cells (*Fig. 4B*), as previously reported (31). This aortic sprouting was significantly influenced by age in control conditions. After 3 days of culture, the capillary network is little developed and similar in 3 and 24 mo rings. In contrast, after 6 days of culture, the length of microvessels was reduced in 24 mo rings (-25.3% *vs.* 3 mo rings) (*Fig. 4A* and *4D*).

Administration of $rhVEGF_{165}$ increased endothelial cell proliferation and microvessel outgrowth in 3 and 24 mo rings as compared to controls (*Fig. 4*). Recombinant $hVEGF_{165}$ at 5ng/mL strongly increased endothelial cell proliferation at day 3, but in a greater extent in 24 mo (+206%) than in 3 mo rings (+112%) (*Fig. 4A* and *4C*). However, such increase in endothelial cell proliferation in 24 mo rings was not associated with capillary growth since capillary network after 3 days of culture remained

Table 1: Cardiac aging was associated with left ventricular hypertrophy and heart failure.

	3 mo	24 mo	28 mo	32 mo
Cardiac hypertrophy				
LV weight/RV weight	3.41±0.09	3.38±0.13	4.17±0.16†	4.75±0.20‡§
LV hemodynamics				
LVSP (mmHg)	129±6	125±7	108±4*†	90±6*‡§
LVEDP (mmHg)	4.7±0.9	4.9±1.4	8.5±1.0*†	12.0±0.5*‡§
+LVdP/dt (mmHg/s)	5975±630	5258±385	2710±150*†	1977±323*‡§
- LVdP/dt (mmHg/s)	4794±432	4431±281	2632±176*†	1807±212*‡§

LV weight/RV weight: left ventricular weight/right ventricular weight; LVSP: left ventricular systolic pressure; LVDP: left ventricular end diastolic pressure; +LVdP/dt and –LVdP/dt: positive and negative first derivative for maximal rates of left ventricular pressure development in 3, 24, 28 and 32 mo rats. Data are expressed as mean±S.E.M.; *P<0.05 *vs*. 3 mo, †P<0.05 28 mo *vs.* 24 mo, ‡P<0.01 32 mo *vs.* 28 mo, §P<0.01 24 mo *vs.* 32 mo.

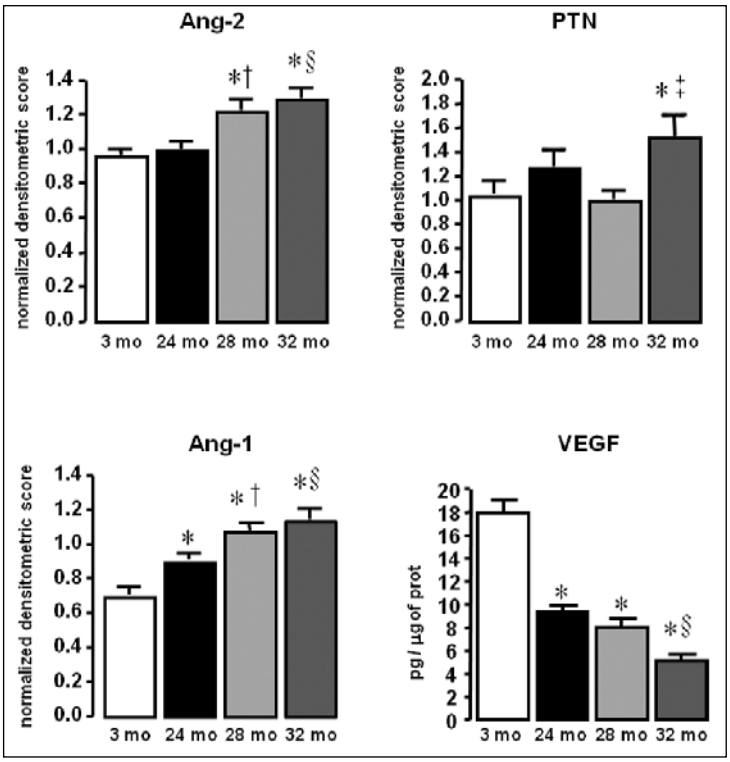

Fig. 2. Age-dependent alterations in growth factors. Ang-2, PTN, Ang-1 and VEGF protein contents in LV from 3, 24, 28 and 32 mo rats. Values are mean±S.E.M. *P<0.05 *vs.* 3 mo, † P<0.05 28 mo *vs.* 24 mo, ‡ P<0.01 32 mo *vs.* 28 mo, § P<0.01 24 mo *vs.* 32 mo.

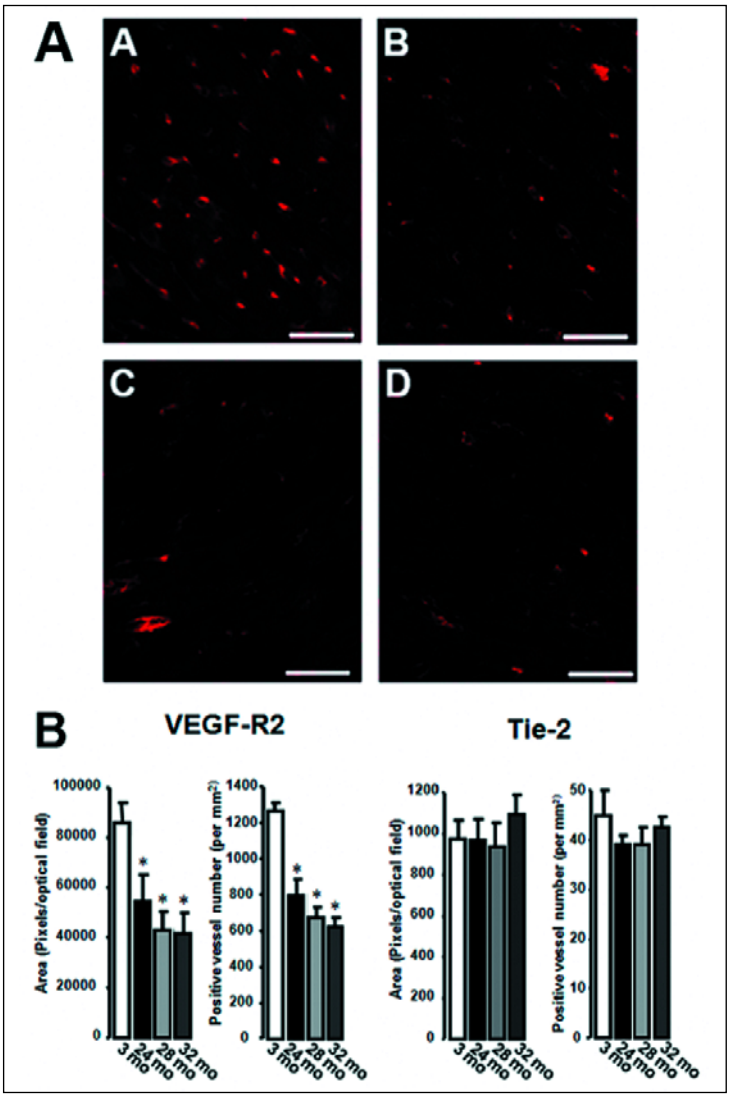

Fig. 3. Age-dependent alterations in VEGFR-2 and Tie2 receptors. Panel A: representative micrographs of immunohistological stainings of VEGF-R2 in 3 (A), 24 (B), 28 (C) and 32 (D) mo LV, obtained under rhodamine filter system. Bar: 20 µm. Panel B: LV content of VEGF-R2 and Tie-2 receptors in 3, 24, 28 and 32 mo rats. The area corresponding to that covered by VEGF-R2 and Tie-2 receptors was quantified by image analysis and expressed as a percentage of the total area. Values are mean±S.E.M. *P<0.05 *vs.* 3 mo.

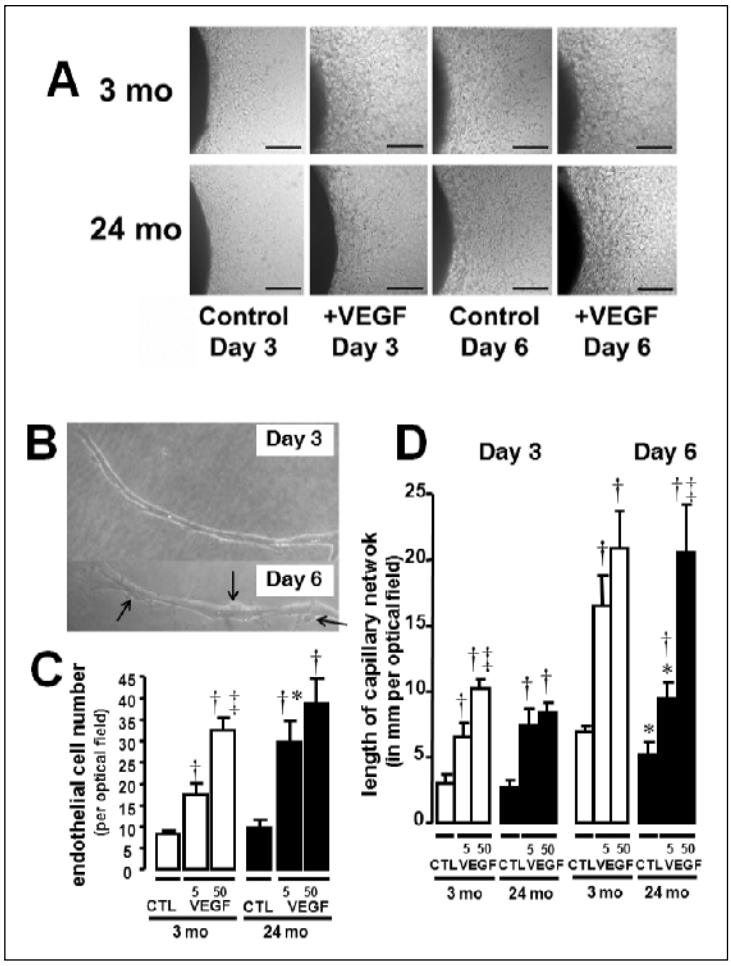

Fig. 4. Capillary outgrow in cultured aortic rings after VEGF treatment. Panel A: representative micrograph of capillary outgrowth in 3 and 24 mo rings in culture with or without rhVEGF$_{165}$ (50 ng/mL) in 3-dimensional collagen gels. Bar: 500 µm. Panel B: high magnification of typical formed microvessels constituted by endothelial tube and surrounding mural cells (arrows) after 3 and 6 days of culture. Panel C and D: endothelial cell proliferation after 3 days and capillary outgrowth after 3 and 6 days of culture respectively in 3-dimensional collagen gels in control (CTL) conditions or after addition of 5 ng/mL or 50 ng/mL of rhVEGF$_{165}$ (VEGF). Values are mean±S.E.M. *P<0.05 *vs.* treatment-matched group, †P<0.001 *vs.* age-matched control group; ‡ P<0.01 treatment with 50 *vs.* 5 ng/mL rhVEGF$_{165}$.

reduced compared to 3 mo rings (*Fig. 4A* and *4D*). In contrast, with higher dose of rhVEGF$_{165}$ (50 ng/mL), endothelial cell number at day 3 (*Fig. 4C*) or at day 6 (63±9 *vs*. 70±6 cells/optical field in 3 mo group, NS) as well as length of capillary network after at day 6 (*Fig. 4D*) were similar in 3 and 24 mo rings. In aged rings, 50 ng/ml of VEGF is able to stimulate endothelial cell proliferation and microvessel formation and to induce a capillary outgrowth similar to that observed in 3 mo rings with the same treatment.

Age-dependent decrease in coronary microvessel density in vivo restored by rhVEGF$_{165}$ therapy

In control conditions, capillary density, detected by vWF immunostaining, was reduced in 24 mo hearts compared to 3 mo hearts (*Fig. 5*), confirming age-dependent decrease in capillary vascular bed. Seven days after treatment, rhVEGF$_{165}$ increased capillary density at both 3 and 24 mo groups (*Fig. 5*). Twenty-one days after treatment, rhVEGF$_{165}$ further increased capillary density in 24 mo treated group leading to similar increase in capillary density in 3 and 24 mo hearts (+30% and +40% *vs.* age-matched control group respectively) after 21 days of treatment. Since numerous isolated vWF positive cells *i.e*. endothelial cells were observed in 3 mo- and 24 mo-VEGF myocardium seven days after treatment, each being counted as a capillary as indicated in Material and Methods, we also quantitated endothelial cell area to complete determination of the extent of angiogenesis. Recombinant hVEGF$_{165}$ also induced an increase in endothelial cell area both at day 7 and 21 in 3 and 24 mo hearts (*Fig. 5*). Arteriolar density was unchanged by rhVEGF$_{165}$ therapy at day 7 but was increased at day 21 at both ages (*Fig. 6*). However this increase was lower in 24 mo-VEGF than in 3 mo-VEGF hearts (*Fig. 6*). rhVEGF$_{165}$ treatment is able to promote new vessel formation in 24 mo hearts, as soon as 7 days after treatment for capillaries and 21 days after treatment for arterioles.

Using *in vivo* SPECT imaging, significant ^{99m}Tc-RAFT-RGD activity was detected in the LV free wall in 3 and 24 mo-VEGF hearts as soon as 7 days after treatment (*Fig. 7*), in contrast to age-matched controls. The LV/S activity ratio remained elevated at day 21 (1.75±0.11 and 1.66±0.12 in 3 and 24 mo-VEGF hearts, NS *vs.* values at day 7), indicating a sustained myocardial uptake of the $\alpha_v\beta_3$ integrin-targeted tracer. Such accumulation of the $\alpha_v\beta_3$ integrin-targeted tracer in VEGF-treated hearts, which was not observed in control hearts in spite of similar inflammatory reaction, assessed by CD-68 and CD-163 immunofluorescence labeling (data not shown), into and around the injection site after both 7 and 21 days of treatment, can therefore not be attributed to an inflammatory cell uptake. In addition, *in situ* fluorescence staining of perfused capillaries showed that the number of microvessels detected after FITC-labeled lectin perfusion was increased 7 days after rhVEGF$_{165}$ treatment in 3 and 24 mo hearts and this improvement in microvessel density persisted at day 21 (*Fig. 8*). A single intramyocardial injection of rhVEGF$_{165}$ is able to induce functional angiogenesis in 3 but also in 24 mo hearts.

DISCUSSION

Age-dependent impairment of angiogenesis has been demonstrated in peripheral and cardiac vascular beds (5, 11) and may contribute to the increased severity of cardiovascular

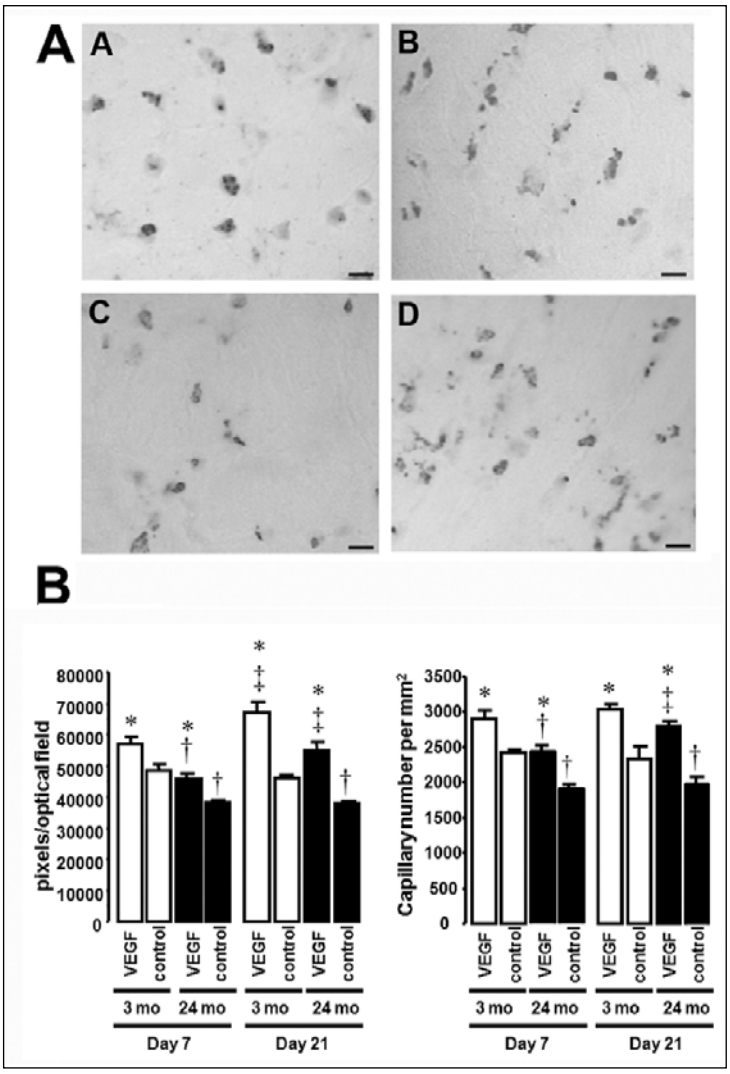

Fig. 5. Capillary density and endothelial cell area after *in vivo* rhVEGF$_{165}$ therapy. Panel A: representative micrographs of immunohistological stainings of vWF in 3 mo-control (A), 3 mo-VEGF (B), 24 mo-control (C) and 24 mo-VEGF (D) LV, 21 days after treatment. Bar 10 μm. Panel B: quantification of number and area of coronary capillaries after 7 and 21 days of treatment in 3 and 24 mo-control and 3 and 24 mo-VEGF rat myocardium. Values are mean±S.E.M. *P<0.01 *vs.* age-matched control group; †P<0.05 *vs.* corresponding treatment-matched group; ‡P<0.05 *vs.* age- and treatment-matched group at day 7.

diseases in the geriatric population. The present study confirms these previous observations and identifies VEGF/VEGF-R2 as the main pathway impaired during aging and age-associated heart failure. It also shows that this age-related attenuation of the protective mechanism of neoangiogenesis can be reversed by rhVEGF$_{165}$ therapy.

Different angiogenic growth factors/receptor regulatory systems, especially balanced Ang-1/Ang-2/Tie-2 and VEGF/VEGF-R2 systems which are critical for the maintenance of vascular integrity, have been extensively studied in different pathological models such as diabetes (32) or myocardial infarction (33). Surprisingly few is known concerning the age-associated changes in these systems involved in cardiac angiogenesis. At 24 months of age, the coronary capillary density and subsequent perfusion are severely impaired (17, 20, 34). At this age, we observed a downregulation of VEGF/VEGF-R2 system associated with a small increase in Ang-1 without change in Ang-2. Ang-1 is a proangiogenic factor that promotes Tie-2 phosphorylation leading to endothelial cell survival, vessel stabilization and then angiogenesis, while Ang-2 induces destabilization of vessels, detachment of pericytes, and degradation of extracellular matrix (35). However, the Ang-1/Ang-2 ratio, which regulates blood vessel sprouting (32), remained unchanged as well as Tie-2 levels at this age which suggest that age-associated impairment of cardiac angiogenesis results mainly from severe downregulation of cardiac VEGF/VEGF-R2 pathway. Previous studies in other rat strains also reported an age-associated decrease in VEGF and VEGF-R2 protein levels (16, 17). However the present study can not determine if the decrease in VEGF came before, followed or was concomitant to the decrease in VEGF-R2 density during aging. Indeed it is well known that VEGF was able to induce *in vitro* expression of VEGF-R2 (36) and that increase in VEGF mRNAs after exercise training came before the increase in VEGF-R2 mRNA in skeletal muscle (37). However a kinetic of VEGF and VEGF-R2 protein quantification is clearly needed between 3 and 24 months of age to precise regulation of VEGF/VEGF-R2 system during cardiac aging. At older ages, *i.e.* 28 and 32 mo, a heart failure appeared, characterized by a severe LV hypertrophy and an increase in LV end diastolic pressure at rest. At this very old age, VEGF and VEGF-R2 levels were at their lower level while all others growth factors quantified *i.e.* Ang-1, Ang-2 and PTN were at their maximum. In models of heart failure in adult rats, inhibition of angiogenesis by a VEGF trap reagent or by a decoy VEGF receptor diminished pressure overload cardiac hypertrophy and capillary density and promoted the progression to heart failure (38). Consequently, VEGF seems to be required to maintain myocardial capillary density and reductions in the coronary bed may lead to transition from compensatory hypertrophy to failure (39). Failure to maintain expression of VEGF and its receptor VEGF-R2 in aged hearts may result in

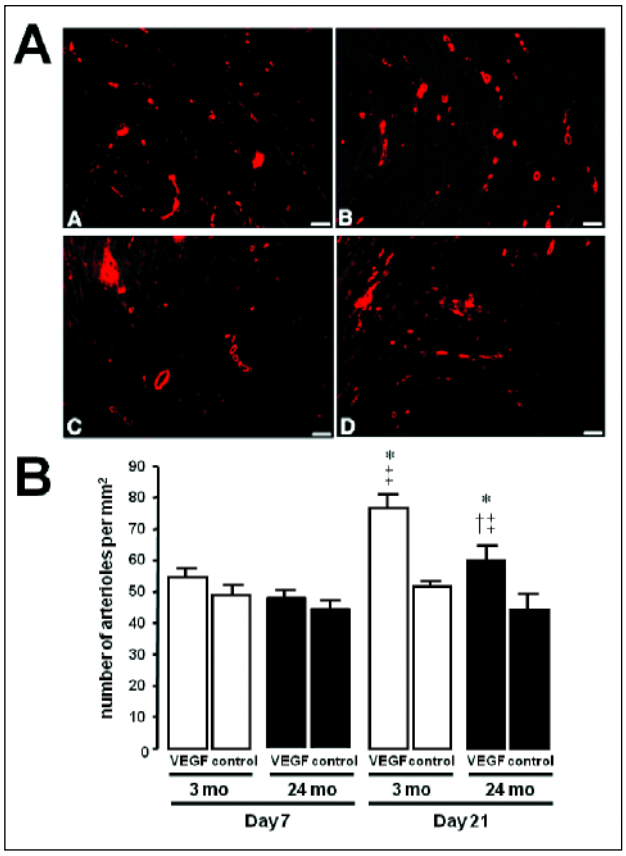

Fig. 6. Arteriolar density after *in vivo* rhVEGF$_{165}$ therapy. Panel A: representative micrographs of immunohistological stainings of α smooth muscle actin in 3 mo-control (A), 3 mo-VEGF (B), 24 mo-control (C) and 24 mo-VEGF (D) left ventricles, 21 days after treatment. Bar 100 µm. Panel B: quantification of arterioles after 7 and 21 days of treament in 3 and 24 mo-control and 3 and 24 mo-VEGF rat myocardium. Values are mean±S.E.M. *P<0.01 *vs.* age-matched control group; †P<0.01 *vs.* corresponding treatment-matched group; ‡P<0.05 *vs.* age- and treatment- matched group at day 7.

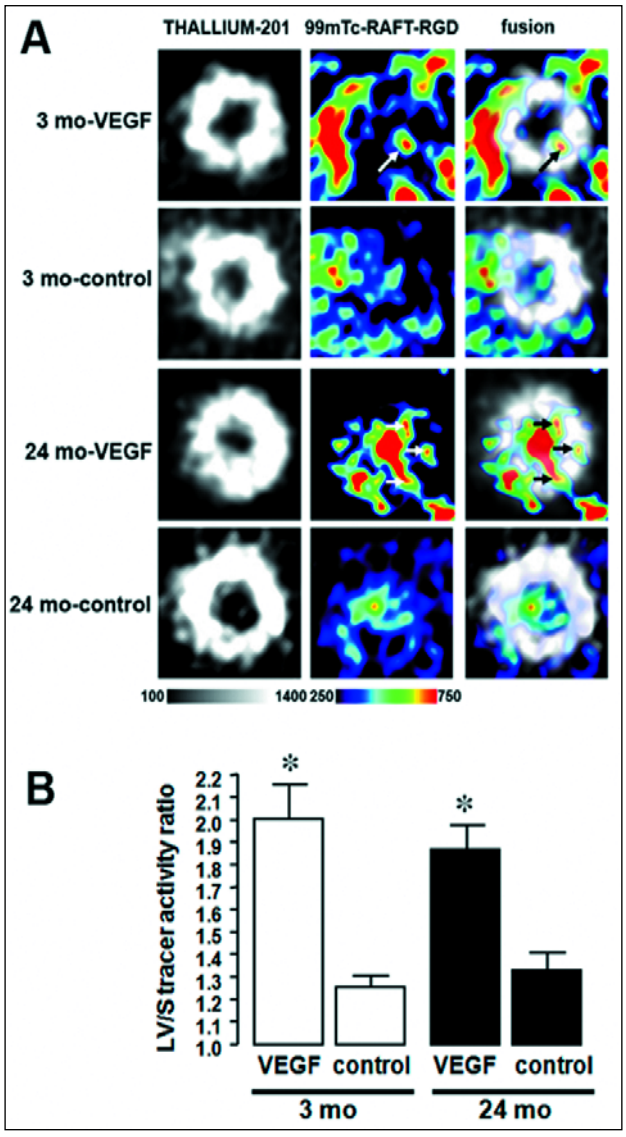

Fig. 7. In vivo functional angiogenesis quantified by noninvasive dual-isotope imaging. Panel A: representative dual-isotope short-axis myocardial slices from tomographic images of the perfusion tracer Thallium-201 and the $\alpha_v\beta_3$ integrin-targeted tracer ^{99m}Tc-RAFT-RGD activities, in 3 mo-control, 3 mo-VEGF, 24 mo-control and 24 mo-VEGF hearts at day 7. The hot spots of $\alpha_v\beta_3$ integrin-targeted tracer ^{99m}Tc-RAFT-RGD (arrows) show a functional angiogenesis in the LV free wall. Panel B: quantification of LV/S ratios from short-axis slices (tomographic) at day 7 after treatment in 3 and 24 mo-control and 3 and 24 mo-VEGF LV. Values are mean±S.E.M. *P<0.01 *vs*. age-matched control group.

the impairment of angiogenesis and then further contribute to the progression to heart failure observed at 28 and 32 mo.

VEGF is the most important growth factor in angiogenesis and a key regulator of blood vessel formation which promotes many of the events required for angiogenesis: proliferation and migration of endothelial cells, remodeling of the extracellular matrix, formation of capillary tubules, and vascular leakage (7, 12). Consequently VEGF plays a critical role in both physiological and pathological angiogenesis. VEGF binds to two types of tyrosine kinase receptors: VEGFR-1, whose role in angiogenesis is controversial and VEGFR-2, which is considered as the major effector of the trophic and permeability actions of VEGF (13, 40). However, the specific role of VEGF in the age-associated decrease in coronary capillaries has not been clearly demonstrated. We hypothesized that VEGF therapy with recombinant growth factor could improve aging-induced downregulation of angiogenesis and tested this hypothesis in *in vitro* and *in vivo* models of angiogenesis in 3 and 24 mo rats.

In vitro assays of angiogenesis are critical to study vascular morphogenesis and to evaluate therapeutic compounds that may promote or inhibit vascular growth. Culture of explanted aortic segments from rats or mice in a 3-dimensional extracellular matrix is one of the most effective ways to generate *in vitro* capillary-like endothelial sprouts (24). We observed that aortic rings from 3 mo rats produced microvessels faster and in greater number than aortic rings from 24 mo rats in the presence of 10% fetal calf serum and in the absence of exogenous growth factors. These results are in agreement with previous studies in aortic rings from aged rodents (31, 41). However rhVEGF$_{165}$ supplementation in the culture medium strongly improved capillary formation, even with low dose of VEGF and in 24 mo rings. This improvement in capillary outgrow is however lower in 24 mo rings than in 3 mo rings but did not result from an impairment in endothelial cell proliferation suggesting that others steps such as endothelial cell adhesion and capillary-like tube formation are implicated in this age-associated delay in

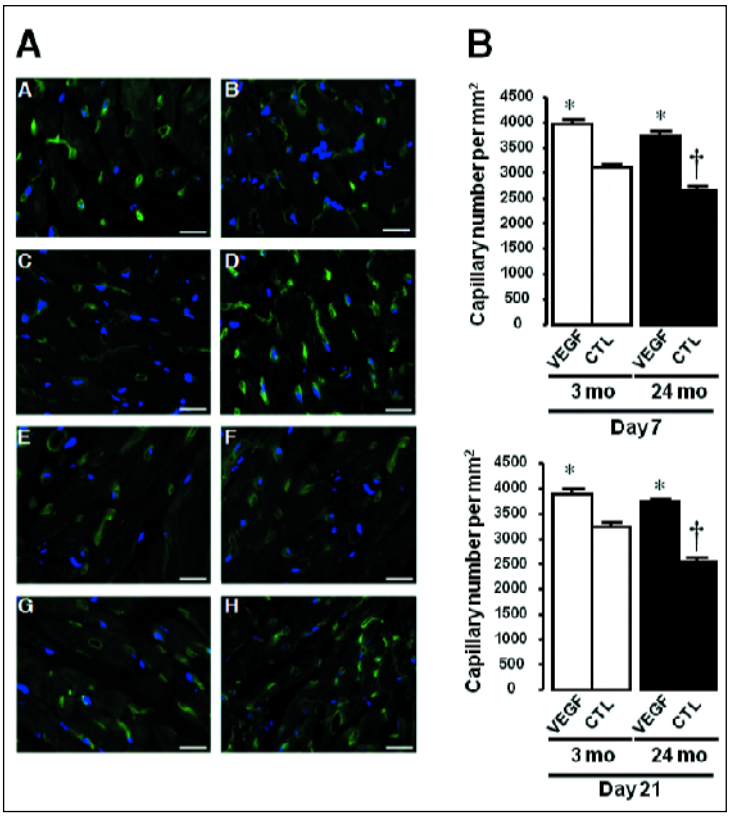

Fig. 8. In situ labeling of capillaries with lectin-FITC after *in vivo* rhVEGF$_{165}$ therapy. Panel A: representative micrographs of immunofluorescence stainings of lectin-FITC in LV from 3 mo-control (A; C), 3 mo-VEGF (B; D), 24 mo-control (E; G) and 24 mo-VEGF (F; H) hearts, 7 and 21 days after treatment respectively. Bar: 10 µm. Panel B: quantification of lectin-FITC labeled vessels after 7 and 21 days of treatment in 3 and 24 mo-control and 3 and 24 mo-VEGF LV. Values are mean±S.E.M. *P<0.01 *vs.* age-matched control group; †P<0.01 *vs.* corresponding treatment-matched group.

angiogenesis. Only one study previously investigated the age-associated effects of VEGF treatment in such model of aortic explants and reported that angiogenic sprouting in response to VEGF and FGF-2 was delayed and associated with a marked reduction in vessel number in middle-aged mice as compared to adults (31). Our present study also demonstrates that rhVEGF$_{165}$ is able to restore angiogenic sprouting in explanted aortic segments from 24 mo rats. However, capillary-like tube formation was only similar at both ages with the higher dose of VEGF and after 6 days of treatment, suggesting that both time and VEGF concentration are important for vessel assembly and vascular leakage. Supplementary studies such as quantification of VEGF-R2 receptors but also VEGF-R2 intracellular signaling (42), and MMPs expression and activity (43) are clearly required to identify mechanisms of this delay in angiogenesis in 24 mo rings.

In vitro angiogenesis in aortic segments is very different from *in vivo* angiogenesis of coronary capillaries in myocardium and consequently studying *in vivo* therapy with VEGF in senescent rats was mandatory. It is well known that aging is associated with coronary dysfunction (2, 34) and consequently angiogenesis, or the sprouting of new blood vessels from a preexisting capillary network, is essential for the repair of aged heart tissue and the preservation of cardiac function. The potential importance of coronary angiogenesis was highlighted by observations that downregulation of VEGF$_{165}$ was involved in the decrease in capillary density observed in patients with dilated cardiomyopathy (38). The administration of recombinant VEGF protein or gene into ischemic myocardium demonstrated beneficial functional and coronary perfusion effects in adult animal models of ischemic heart disease (14, 44), as well as in patients with severe myocardial ischemia (45). However, the *in vivo* safety of this therapy remains a major concern. Indeed unregulated continuous expression of VEGF, leading to excessive VEGF at injection sites, led to the formation of angioma at the site of injection (46) while systemic injection induced adverse effects such as hypotension (47). Besides, clinical studies using VEGF gene therapy failed to demonstrate any benefit for coronary perfusion or myocardial function (48). In contrast, fewer clinical trials with VEGF protein reported improvement of myocardial perfusion at rest and improvement in angina 120 days after the therapy (45, 49). Consequently, research efforts have turned toward the local delivery of angiogenic factors *i.e.* protein therapy at low doses. In rabbit adult heart, therapy with low doses (10 µg) of recombinant VEGF$_{165}$ and FGF-2 was able to induce angiogenesis after myocardial infarction (15). Because the angiogenic effect of VEGF is strongly dependent on its local concentration (48), the delicate control of a protein VEGF therapy, both in dosage and localization, is important to decrease its possible adverse effects, but also to observe therapeutic efficiency, especially in senescent hearts. Indeed, in senescent mice, pinnal injection of 100 ng VEGF$_{165}$ failed to neovascularize the transplanted cardiac allografts (11). However Bougioukas *et al*. (15) reported that 5 µg VEGF induced lower increase in vascular density than 10 µg. Consequently the failure of VEGF-induced angiogenesis in the transplanted cardiac allografts (11) could be explained by the too low dose of VEGF165 used (100 ng). In the present study we have chosen a protein therapy with VEGF165, a growth factor which can stably binds to fibronectin and heparan sulfate of extracellular matrix (50, 51). VEGF$_{165}$ was administrated at the dose of 10 µg, previously used with success in adult rat after myocardial infarction (26), in both adult and senescent hearts by intramyocardial injections since local delivery of agents ensured high myocardial uptake. We found that such treatment was efficient to induce capillary growth *i.e.* angiogenesis, as soon as 7 days after treatment but also collateral artery growth *i.e.* arteriogenesis, after 21 days of treatment at both ages. A successful vascular growth therapy comprises angiogenesis but also arteriogenesis, both being necessary to enhance coronary blood flow. Moreover, *in vivo* nuclear imaging indicated an

accumulation of the $\alpha_v\beta_3$ integrin-targeted tracer ^{99m}Tc-RAFT-RGD as soon as day 7 which was persistent at day 21. Such $\alpha_v\beta_3$ integrin-trageted tracer accumulation has been previously used to detect angiogenesis by nuclear imaging in a myocardial infarction model (29). Although the endothelial cell population is predominant among the cardiac cellular population expressing $\alpha_v\beta_3$ integrin, migrating alpha smooth muscle cells also expressed $\alpha_v\beta_3$ integrin (52). Consequently the $\alpha_v\beta_3$ integrin-targeted tracer uptake labeled both endothelial and alpha smooth muscle cells *i.e.* angiogenesis and arteriogenesis Such *in vivo* accumulation of the $\alpha_v\beta_3$ integrin-targeted tracer ^{99m}Tc-RAFT-RGD and *ex vivo* labeling of vessels with FITC-lectin after 7 and 21 days of treatment clearly showed that such new capillaries and arterioles were well perfused, indicating functional angiogenesis and arteriogenesis. However, molecular and cellular mechanisms induced by VEGF administration and leading to observed angiogenesis and arteriogenesis remain to be determined as well as potential protective effect of such therapy in heart failure associated to advanced age and/or after ischemic cardiac diseases.

In the present study we demonstrated that intramyocardial administration of rhVEGF$_{165}$ protein at low doses enhances neoangiogenesis in the senescent myocardium. This result broadens the concept of effective therapeutic angiogenesis at low doses in the senescent myocardium, avoiding the use of high circulating levels of growth factors that could potentially induce deleterious adverse effect. The model of intramyocardial injection may, of course, be a limitation in the applicability of the technique but in the clinical setting, a catheter-based percutaneous technique has been developed for nonsurgical intramyocardial growth factor gene therapy, minimizing the attendant risks of surgery (53).

Acknowledgements: The authors thank Dr Claude Sebban and Brigitte Decros for kindly providing aged rats and Rene Bontron for meticulous care and handling of the rats. This work was supported by grants from Fondation de France and Association Française contre les Myopathies.

Conflict of interests: None declared.

REFERENCES

1. Masoudi FA, Havranek EP, Krumholz HM. The burden of chronic congestive heart failure in older persons: magnitude and implications for policy and research. *Heart Fail Rev* 2002; 7: 9-16.
2. Hachamovitch R, Wicker P, Capasso JM, Anversa P. Alterations of coronary blood flow and reserve with aging in Fischer 344 rats. *Am J Physiol* 1989; 256: H66-H73.
3. Besse S, Bulteau AL, Boucher F, Riou B, Swynghedauw B, de Leiris J. Antioxidant treatment prevents cardiac protein oxidation after ischemia-reperfusion and improves myocardial function and coronary perfusion in senescent hearts. *J Physiol Pharmacol* 2006; 57: 541-552.
4. Goldspink DF, Burniston JG, Tan LB. Cardiomyocyte death and the ageing and failing heart. *Exp Physiol* 2003; 88: 447-458.
5. Edelberg JM, Reed MJ. Aging and angiogenesis. *Front Biosci* 2003; 8: s1199-s1209.
6. Ahluwalia A, Li A, Cheng G, Deng X, Tarnawski AS. Reduced ghrelin in endothelial cells plays important mechanistic role in aging-related impairment of angiogenesis. *J Physiol Pharmacol* 2009; 60(2): 29-34.
7. Yancopoulos GD, Davis S, Gale NW, Rudge JS, Wiegand SJ, Holash J. Vascular-specific growth factors and blood vessel formation. *Nature* 2000; 407: 242-248.
8. Christman KL, Fang Q, Kim AJ, *et al*. Pleiotrophin induces formation of functional neovasculature in vivo. *Biochem Biophys Res Commun* 2005; 332: 1146-1152.
9. Tomanek RJ, Zheng W, Yue X. Growth factor activation in myocardial vascularization: therapeutic implications. *Mol Cell Biochem* 2004; 264: 3-11.
10. Friehs I, Moran AM, Stamm C, *et al*. Promoting angiogenesis protects severely hypertrophied hearts from ischemic injury. *Ann Thorac Surg* 2004; 77: 2004-2010; discussion: 2011.
11. Edelberg JM, Lee SH, Kaur M, *et al*. Platelet-derived growth factor-AB limits the extent of myocardial infarction in a rat model: feasibility of restoring impaired angiogenic capacity in the aging heart. *Circulation* 2002; 105: 608-613.
12. Maulik N, Thirunavukkarasu M. Growth factors and cell therapy in myocardial regeneration. *J Mol Cell Cardiol* 2008; 44: 219-227.
13. Gille H, Kowalski J, Li B, *et al*. Analysis of biological effects and signaling properties of Flt-1 (VEGFR-1) and KDR (VEGFR-2). A reassessment using novel receptor-specific vascular endothelial growth factor mutants. *J Biol Chem* 2001; 276: 3222-3230.
14. Banai S, Jaklitsch MT, Shou M, *et al.* Angiogenic-induced enhancement of collateral blood flow to ischemic myocardium by vascular endothelial growth factor in dogs. *Circulation* 1994; 89: 2183-2189.
15. Bougioukas I, Didilis V, Ypsilantis P, *et al*. Intramyocardial injection of low-dose basic fibroblast growth factor or vascular endothelial growth factor induces angiogenesis in the infarcted rabbit myocardium. *Cardiovasc Pathol* 2007; 16: 63-68.
16. Xaymardan M, Zheng J, Duignan I, *et al.* Senescent impairment in synergistic cytokine pathways that provide rapid cardioprotection in the rat heart. *J Exp Med* 2004; 199: 797-804.
17. Iemitsu M, Maeda S, Jesmin S, Otsuki T, Miyauchi T. Exercise training improves aging-induced downregulation of VEGF angiogenic signaling cascade in hearts. *Am J Physiol Heart Circ Physiol* 2006; 291: H1290-H1298.
18. Zheng J, Chin A, Duignan I, Won KH, Hong MK, Edelberg JM. Growth factor-mediated reversal of senescent dysfunction of ischemia-induced cardioprotection. *Am J Physiol Heart Circ Physiol* 2006; 290: H525-H530.
19. Swynghedauw B, Besse S, Assayag P, *et al*. Molecular and cellular biology of the senescent hypertrophied and failing heart. *Am J Cardiol* 1995; 76: 2D-7D.
20. Assayag P, Charlemagne D, de Leiris J, *et al*. Senescent heart compared with pressure overload-induced hypertrophy. *Hypertension* 1997; 29: 15-21.
21. Plouet J, Moro F, Bertagnolli S, *et al*. Extracellular cleavage of the vascular endothelial growth factor 189-amino acid form by urokinase is required for its mitogenic effect. *J Biol Chem* 1997; 272: 13390-13396.
22. Le Page C, Noirez P, Courty J, Riou B, Swynghedauw B, Besse S. Exercise training improves functional post-ischemic recovery in senescent heart. *Exp Gerontol* 2009; 44: 177-182.
23. Vacherot F, Delbe J, Heroult M, Barritault D, Fernig DG, Courty J. Glycosaminoglycans differentially bind HARP and modulate its biological activity. *J Biol Chem* 1999; 274: 7741-7747.
24. Zhu WH, Nicosia RF. The thin prep rat aortic ring assay: a modified method for the characterization of angiogenesis in whole mounts. *Angiogenesis* 2002; 5: 81-86.
25. Post MJ, Laham R, Sellke FW, Simons M. Therapeutic angiogenesis in cardiology using protein formulations. *Cardiovasc Res* 2001; 49: 522-531.

26. Zhang J, Ding L, Zhao Y, *et al*. Collagen-targeting vascular endothelial growth factor improves cardiac performance after myocardial infarction. *Circulation* 2009; 119: 1776-1784.
27. Sancey L, Ardisson V, Riou LM, *et al.* In vivo imaging of tumour angiogenesis in mice with the alpha(v)beta (3) integrin-targeted tracer 99mTc-RAFT-RGD. *Eur J Nucl Med Mol Imaging* 2007; 34: 2037-2047.
28. Dor Y, Djonov V, Keshet E. Induction of vascular networks in adult organs: implications to proangiogenic therapy. *Ann NY Acad Sci* 2003; 995: 208-216.
29. Dimastromatteo J, Riou LM, Ahmadi M, *et al*. In vivo molecular imaging of myocardial angiogenesis using the alpha(v)beta3 integrin-targeted tracer 99mTc-RAFT-RGD. *J Nucl Cardiol* 2010; 17: 435-443.
30. Uchida N, Nagai K, Sakurada Y, Shirota K. Distribution of VEGF and flt-1 in the normal dog tissues. *J Vet Med Sci* 2008; 70: 1273-1276.
31. Zhu WH, Iurlaro M, MacIntyre A, Fogel E, Nicosia RF. The mouse aorta model: influence of genetic background and aging on bFGF- and VEGF-induced angiogenic sprouting. *Angiogenesis* 2003; 6: 193-199.
32. Tuo QH, Zeng H, Stinnett A, *et al.* Critical role of angiopoietins/Tie-2 in hyperglycemic exacerbation of myocardial infarction and impaired angiogenesis. *Am J Physiol Heart Circ Physiol* 2008; 294: H2547-H2557.
33. Sandhu R, Teichert-Kuliszewska K, Nag S, *et al.* Reciprocal regulation of angiopoietin-1 and angiopoietin-2 following myocardial infarction in the rat. *Cardiovasc Res* 2004; 64: 115-124.
34. Anversa P, Li P, Sonnenblick EH, Olivetti G. Effects of aging on quantitative structural properties of coronary vasculature and microvasculature in rats. *Am J Physiol* 1994; 267: H1062-H1073.
35. Thomas M, Augustin HG. The role of the angiopoietins in vascular morphogenesis. *Angiogenesis* 2009; 12: 125-137.
36. Shen BQ, Lee DY, Gerber HP, Keyt BA, Ferrara N, Zioncheck TF. Homologous up-regulation of KDR/Flk-1 receptor expression by vascular endothelial growth factor in vitro. *J Biol Chem* 1998; 273: 29979-29985.
37. Lloyd PG, Prior BM, Yang HT, Terjung RL. Angiogenic growth factor expression in rat skeletal muscle in response to exercise training. *Am J Physiol Heart Circ Physiol* 2003; 284: H1668-H1678.
38. Shiojima I, Sato K, Izumiya Y, *et al.* Disruption of coordinated cardiac hypertrophy and angiogenesis contributes to the transition to heart failure. *J Clin Invest* 2005; 115: 2108-2118.
39. Hoenig MR, Bianchi C, Rosenzweig A, Sellke FW. The cardiac microvasculature in hypertension, cardiac hypertrophy and diastolic heart failure. *Curr Vasc Pharmacol* 2008; 6: 292-300.
40. Toyota E, Matsunaga T, Chilian WM. Myocardial angiogenesis. *Mol Cell Biochem* 2004; 264: 35-44.
41. Arthur WT, Vernon RB, Sage EH, Reed MJ. Growth factors reverse the impaired sprouting of microvessels from aged mice. *Microvasc Res* 1998; 55: 260-270.
42. Holmes K, Roberts OL, Thomas AM, Cross MJ. Vascular endothelial growth factor receptor-2: structure, function, intracellular signalling and therapeutic inhibition. *Cell Signal* 2007; 19: 2003-2012.
43. Davis GE, Saunders WB. Molecular balance of capillary tube formation versus regression in wound repair: role of matrix metalloproteinases and their inhibitors. *J Investig Dermatol Symp Proc* 2006; 11: 44-56.
44. Ferrarini M, Arsic N, Recchia FA, *et al*. Adeno-associated virus-mediated transduction of VEGF165 improves cardiac tissue viability and functional recovery after permanent coronary occlusion in conscious dogs. *Circ Res* 2006; 98: 954-961.
45. Hendel RC, Henry TD, Rocha-Singh K, *et al.* Effect of intracoronary recombinant human vascular endothelial growth factor on myocardial perfusion: evidence for a dose-dependent effect. *Circulation* 2000; 101: 118-121.
46. Lee RJ, Springer ML, Blanco-Bose WE, Shaw R, Ursell PC, Blau HM. VEGF gene delivery to myocardium: deleterious effects of unregulated expression. *Circulation* 2000; 102: 898-901.
47. Epstein SE, Kornowski R, Fuchs S, Dvorak HF. Angiogenesis therapy: amidst the hype, the neglected potential for serious side effects. *Circulation* 2001; 104: 115-119.
48. Yla-Herttuala S, Rissanen TT, Vajanto I, Hartikainen J. Vascular endothelial growth factors: biology and current status of clinical applications in cardiovascular medicine. *J Am Coll Cardiol* 2007; 49: 1015-1026.
49. Henry TD, Annex BH, McKendall GR, *et al*. The VIVA trial: vascular endothelial growth factor in ischemia for vascular angiogenesis. *Circulation* 2003; 107: 1359-1365.
50. Park JE, Keller GA, Ferrara N. The vascular endothelial growth factor (VEGF) isoforms: differential deposition into the subepithelial extracellular matrix and bioactivity of extracellular matrix-bound VEGF. *Mol Biol Cell* 1993; 4: 1317-1326.
51. Wijelath ES, Rahman S, Namekata M, *et al.* Heparin-II domain of fibronectin is a vascular endothelial growth factor-binding domain: enhancement of VEGF biological activity by a singular growth factor/matrix protein synergism. *Circ Res* 2006; 99: 853-860.
52. Wilder RL. Integrin alpha V beta 3 as a target for treatment of rheumatoid arthritis and related rheumatic diseases. *Ann Rheum Dis* 2002; 61(Suppl 2): ii96-ii99.
53. Stewart DJ, Kutryk MJ, Fitchett D, *et al*. VEGF gene therapy fails to improve perfusion of ischemic myocardium in patients with advanced coronary disease: results of the NORTHERN trial. *Mol Ther* 2009; 17: 1109-1115.

Received: March 11, 2010
Accepted: November 8, 2010

Author's address: Dr. Sophie Besse, Laboratoire Croissance cellulaire, Reparation et Regeneration tissulaires, EAC CNRS 7149 Faculte des Sciences et Techniques, Universite Paris 12, 61 Avenue du General de Gaulle, 94010 Creteil cedex, France; Phone: 33 1 45171815; Fax: 33 1 45171816; E-mail: Sophie.Besse@parisdescartes.fr